Available online at www.sciencedirect.com

ScienceDirect

Current Opinion in Chemical Biology

SOD mimics: From the tool box of the chemists to cellular studies

Clotilde Policar, Jean Bouvet, Hélène C. Bertrand and Nicolas Delsuc

Abstract

Superoxide dismutases (SODs) are metalloproteins that protect cells against oxidative stress by controlling the concentration of superoxide (O_2^-) through catalysis of its dismutation. The activity of superoxide dismutases can be mimicked by low-molecular-weight complexes having potential therapeutic applications. This review presents recent strategies for designing efficient SOD mimics, from molecular metal complexes to nanomaterials. Studies of these systems in cells reveal that some SOD mimics, designed to react directly with superoxide, may also indirectly enhance the cellular antioxidant arsenal. Finally, a good understanding of the bioactivity requires information on the cell-penetration, speciation, and subcellular location of the SOD mimics: we will describe recent studies and new techniques that open opportunities for characterizing SOD mimics in biological environments.

Addresses

Laboratoire de BioMolécules (LBM), Département de Chimie, Sorbonne Université, École Normale Supérieure, PSL University, Sorbonne Université, CNRS, 75005, Paris, France

Corresponding author: Policar, Clotilde (clotilde.policar@ens.psl.eu)

Current Opinion in Chemical Biology 2022, **67:**102109

This review comes from a themed issue on **Bioinorganic Chemistry (2022)**

Edited by **Emily Que**

For complete overview of the section, please refer to the article collection Bioinorganic Chemistry (2022)

Available online 20 January 2022

https://doi.org/10.1016/j.cbpa.2021.102109

Keywords

SOD mimics or mimetics, Design of metallodrugs, X-fluorescence imaging or X-fluorescence microscopy XFM, Cellular studies.

Abbreviations

BNP/SNP, Boehmite nanoparticles/silica nanoparticles; COVID, Coronavirus disease; cyt *c*, Ferricytochrome *c*; DMSO, Dimethyl sulfoxide; EDTA, Ethylenediaminetetraacetic acid or 2,2',2",2"'-(ethane-1,2-diyldinitrilo)tetraacetic acid; EPR, Electron paramagnetic resonance; H,P, and T, HEPES, phosphate and TRIS buffers; ICP-MS, Inductive-coupled plasma mass spectrometry; IECs, Intestinal epithelial cells; Keap1-nrf2, Kelch-like ECH-associated protein 1 - nuclear factor erythroid 2-related factor 2; LC-MS/MS, Liquid Chromatography coupled with tandem mass spectrometry; MCF, McCord and Fridovich assay; MCM-41, Mesoporous MCM-41 silica; MnPs, Mn-porphyrins; MOF, Metal-organic frameworks; NBT / XTT, Nitro blue tetrazolium / 2,3-bis-(2-methoxy-4-nitro-5-sulfophenyl)-2H-tetrazolium-5-carboxianilide; NHE, Normal Hydrogen Electrode; PAM, Poly-aza-macrocycles; PFA, Paraformaldehyde; PR, Pulsed radiolysis; RNS/ROS, Reactive nitrogen species/reactive oxygen species; SBA-15, Mesoporous SBA-15 silica; SF, Stopped-flow; SOD, Superoxide dismutase; XAS/XFM, X-Ray absorption spectroscopy/X-Ray fluorescence microscopy.

Introduction

Superoxide dismutases (SODs) are metalloproteins involved in the cellular protection against superoxide, a reactive species derived from dioxygen by one-electron reduction. Superoxide (O_2^- [1]) is a metastable radical anion endowed with both signaling and deleterious properties [2,3]. SODs participate in the control of its cellular concentration (about 10 pM in mammalian cells [4]) by catalyzing its dismutation (1), resulting from two monoelectronic processes (2) and (3), with (1) = (2) + (3)

$$2\,O_2^- + 2H^+ \rightarrow O_2 + H_2O_2 \quad (1)$$

$$O_2^- \rightarrow O_2 + e^- \quad (2)$$

$$O_2^- + 2H^+ + e^- \rightarrow H_2O_2 \quad (3)$$

SODs are remarkably efficient proteins that catalyze superoxide dismutation with kinetics only limited by diffusion (ca. 10^9 $mol^{-1}Ls^{-1}$). Four families of SODs use different metallic redox couples, Cu(II/I)−Zn(II), Cu(II/I), Fe(III/II), Mn(III/II) or Ni(III/II) [2,5], with a redox potential in a very narrow range (ca. 0.30 V/NHE) [2,6]. Optimal kinetics is expected for a potential at 0.36 V/NHE [6,7], the mid-point potential [8,9] of the two couples involved in superoxide dismutation ($E°'_{pH7,\ 25°C}(O_{2aq}/O_2^-)$ = −0.18 V/NHE and $E°'_{pH7,\ 25°C}(O_2^-/H_2O_2)$ = 0.91 V/NHE, apparent redox potentials at pH7 and taking into account dioxygen low solubility in water [10]). This pinpoints the redox potential as a key parameter, but electrostatic attraction by a positively charged funnel described for all SODs, except Cu-only SOD in which the Cu active site is open to solvent [11], also contributes to the fast, only diffusion-limited, reaction with superoxide [2]. Oxidative stress, described as an imbalance between the flow of reactive species and protective pathways, is associated with a range of physiopathological conditions. Chemists can take inspiration

from nature to design complexes or materials reproducing SOD activity [6], and that could be used for therapeutic applications [12–14]. These aspects have been extensively reviewed [6,13,15–19] along with the therapeutic applications of SOD mimics [12,14,20,21]. Note that the SOD mimics discussed here are presented in both the Scheme 1 (molecular structures and abbreviations) and Table 1 (physicochemical properties and references), Cp standing for compound and Pep for peptides.

The redox dependence mentioned earlier was not always experimentally observed for SOD mimics, suggesting that other parameters could be key players. Various studies on a range of SOD mimics, with Mn^{II} (Cp22-23, Cp24-28), Cu^{II} (Cp11,14), or Ni^{II} (Pep18), have shown the importance of a coordinated water molecule [8,22–25]. This can be rationalized either by a fast exchange with superoxide, in an inner-sphere electron transfer requiring that superoxide enters the coordination sphere of the metal ion [25] involving a M-OO intermediate, or through the effect of proton donation to the reduced peroxide to lead to H_2O_2 release [26]. Second coordination sphere effects have also been described, revealing a possible fine modulation of the Mn-OO bond's strength upon variation of electronic effects on a Schiff-base ligand (Cp38-43) [27]. The dimerization of monometallic Mn(II) complexes upon reaction with superoxide was also observed [27], a known process leading to Mn(III)–Mn(IV) μ-oxo complexes [6,8] that are 'dead-end' for superoxide dismutation activity. This dimerization process was shown to be prevented by a sterically hindered metal ion environment [8]. Bulky substituents can also favor catalysis by modulating the stability of intermediates of the catalytic cycle (M–OO). Indeed, isopropyl moieties (Cp9) were shown to preclude hydrogen bonds that stabilize a Cu-peroxo intermediate (with Cp10) [28]. This was in favor of catalysis, as a too stable intermediate would disfavor the release of the product (H_2O_2). Several studies of Cu(II) or Mn(II) complexes with cyclic polyamines also suggested structural effects that could finely modulate the SOD-like activity: flexibility of the ligand that would permit molecular rearrangements of the complex along the catalytic pathway [29], or that would favor Mn(II) oxidation to the Jahn-Teller distorted Mn(III) complex [30], in relation to redox tuning.

Below, we describe selected recent strategies for designing efficient SOD mimics and discuss the importance of cell studies to understand, and possibly improve, bioactivity, including the investigation of cellular pathways and of SOD mimics cellular fate with innovative imaging approaches.

New directions in the design of SOD mimics: from low molecular–weight complexes to nanomaterials

Peptide-based complexes

Peptides have been used as ligands to generate metal complexes mimicking the different SOD enzymes. Linear short sequences (Pep4-17) engaged in complexes with Cu^{II} [31,32] or Ni^{II} [33] cations have shown promising intrinsic catalytic activities. To circumvent the high conformational flexibility of peptides that entropically disfavors coordination [34], a cyclic peptide (Pep3) [35] or preorganized peptide scaffolds as *de novo* mini-proteins [36] have been used. A strategy involving the generation of a library of peptides screened with metal ions through an activity-based assay has led to the characterization of a copper complex mimicking SOD (Pep1), efficient even in cellular models of oxidative stress [37]. This strategy has been successfully extended to the discovery of the first peptidyl di-copper(II) complex (Pep2) mimicking the catalase enzyme [38]. Interestingly, depending on the activity assay used for the screening, complexes possessing only the desired activity were selected—desired activity, namely, monoelectronic SOD activity with a mono-metallic peptide complex or bi-electronic catalase activity with a dicopper complex [37,38].

Redox-ligand based SOD mimics

So far, there are no known SODs using an organic redox cofactor, probably because monoelectronic redox processes could lead to reactive radical intermediates. However, Goldsmith et al. have prepared a Zn(II)-complex with a di-hydroxybenzyl ligand (Cp34) Zn^{II}-OPh-OH that could potentially lead to a Zn^{II}-phenoxyl-radical ([Zn^{II}-°OPh-O^- ↔ Zn^{II}-OPh-O°]) [39,40]. This Zn^{II}-phenoxyl radical acted as a SOD mimic, cycling between a Zn^{II}-*para*-quinone and a Zn^{II}-phenoxyl radical. This reactivity is associated with the di-hydroxybenzyl moiety, with its rich monoelectronic chemistry involving radical-phenoxyl and quinone. Whereas Zn^{II} analogs of some Mn^{II} SOD mimics with a bound phenol (Cp29) have been shown to be redox inactive [41–44], the Zn^{II}-OPh-OH complex (Cp34) was found electroactive, with a quasi-reversible wave at 0.35 V/NHE, very close to the optimal redox potential for superoxide dismutation (0.36 V/NHE). Zn^{II} was suggested to play a double role, attracting the anion substrate [45] and facilitating the cycling between the phenoxyl radical and quinone. In 2021, the mechanism of superoxide dismutation was investigated for Mn(II) analogs (Cp35-36) using cryospray-ionization mass spectrometry (CSI-MS), and an intricate mechanism involving quinone intermediates, but also a quinone-Mn^{IV}=O, was beautifully characterized [46].

Nanoparticles

Nanoparticles have been developed, either through the incorporation of known discrete SOD mimics in non-active materials (silica, alumina) or by the use of metal-based materials, including metallic nanoparticles or metal–organic frameworks, in which the basic structural unit can be responsible for antioxidant

Table 1

Names, abbreviations, redox potentials, and catalytic activities of SOD mimics mentioned here.

SOD mimics	Abbreviation	$E_{1/2}$ (mV vs. NHE)	$\log k_{cat}$ ($O_2^{\cdot-}$): $method_{detector}$ (pH) = $\log k_{cat}$(buffer)	References
Porphyrins				
Mn^{III}TE-2-PyP^{5+}	Cp1	+228	$MCF_{cyt\ c}$(7.8) = 7.76 (P)	[20,86]
Mn^{III}TnHex-2-PyP^{5+}	Cp2	+314	$MCF_{cyt\ c}$(7.8) = 7.48 (P)	[20]
Mn^{III}TnBuOE-2-PyP^{5+}	Cp3	+277	$MCF_{cyt\ c}$(7.8) = 7.83 (P)	[12]
$Mn^{III}TBAP^{3-}$	Cp4	–194	$MCF_{cyt\ c}$(7.8) = 3.16 (P)	[20,86]
$Fe^{III}(P^{2+})\ (H_2O)\ (OH)^{4+}$	Cp5	+298	–	[26]
$Mn^{III}(P^{2+})\ (H_2O)_2^{5+}$	Cp6	+270	–	[26]
$Fe^{III}(P^{6+})\ (H_2O)\ (OH)^{8+}$	Cp7	+249	–	[26]
$Mn^{III}(P^{6+})\ (H_2O)_2^{9+}$	Cp8	+200	–	[26]
PAM				
$[Cu^{II}L1(OH_2)]^{2+}$	Cp9	–	MCF_{NBT}(7.4) = 7.14 (T)	[28]
$[Cu^{II}L2(OH_2)]^{2+}$	Cp10	–	MCF_{NBT}(7.4) = 6.86 (T)	[28]
Cu^{II}_2-L3	Cp11	+57	MCF_{NBT}(7.4) = 6.73 (H)	[23]
Cu^{II}_2-BNP-L3	Cp12	–	MCF_{NBT}(7.4) = 7.63 (H)	[23]
Cu^{II}_2-SNP-L3	Cp13	–	MCF_{NBT}(7.4) = 6.09 (H)	[23]
Cu^{II}_2-L4	Cp14	–33	MCF_{NBT}(7.4) = 7.07 (H)	[23]
Cu^{II}_2-BNP-L4	Cp15	–78	MCF_{NBT}(7.4) = 7.56 (H)	[23]
Cu^{II}_2-SNP-L4	Cp16	–	MCF_{NBT}(7.4) = 6.98 (H)	[23]
Mn^{II} pyane	Cp17	–	SF(7.4) = 7.44 (H)/6.92 (P)	[79]
Mn^{II} pyane-pyrene	Cp18	–	SF(7.4) = 6.98 (H)/6.46 (P)	[79]
Mn^{II} pyane-rhodB	Cp19	–	SF(7.4) = 7.08 (H)/6.54 (P)	[79]
Mn^{II} M40403 (Imisopasem)	Cp20	+525	PR(7.4) = 6.55 (P)	[30]
Mn^{II} GC4419 (Avasopasem)	Cp21	–	–	–
Mn^{II} 3,6-PC2A	Cp22	+925	MCF_{NBT}(7.8) = 5.01 (P)	[22]
Mn^{II} 3,9-PC2A	Cp23	+794	MCF_{NBT}(7.8) = 4.29 (P)	[22]
Amine Centered				
$[Mn^{II}(TMIMA)_2]^{2+}$	Cp24	+704	$MCF_{cyt\ c}$(7.8) = 6.56 (P)	[8]
$[Mn^{II}(BMPG)]^{+}$	Cp25	+549	$MCF_{cyt\ c}$(7.8) = 6.68 (P)	[8]
$[Mn^{II}(IPG)]^{+}$	Cp26	+759	$MCF_{cyt\ c}$(7.8) = 6.28 (P) PR(7.8) = 6.58 (P)	[8]
$[Mn^{II}(BIG)]^{+}$	Cp27	+789	$MCF_{cyt\ c}$(7.8) = 6.18 (P) PR(7.8) = 6.15 (P)	[8] [87]
$[Mn^{III}(PI)_2]^{+}$	Cp28	+514	$MCF_{cyt\ c}$(7.8) = 6.82 (P)	[8]
Salans				
$Mn^{II}1^{+}$	Cp29	+440	$MCF_{cyt\ c}$(7.8) = 6.85 (P) SF(7.4) = 6.70(H)	[42] [88]
$Mn^{II}1$-Re^{+}	Cp30	+487	$MCF_{cyt\ c}$(7.8) = 6.81 (P) SF(7.8) = 6.81 (M)	[42]
$Mn^{II}1$-R_9^{10+}	Cp31	+419	SF(7.4) = 6.70 (H)	[43]
$Mn^{II}1$-RW_9^{7+}	Cp32	–	SF(7.4) = 7.24 (H)	[43]
$Mn^{II}1$-MPP^{3+}	Cp33	+404	SF(7.4) = 7.34 (H)	[43]
$[Zn^{II}(Hqp1)]^{+}$	Cp34	+305	SF(7.4) = 6.53 (H)/7.28 (P)	[39]
$[Mn^{II}(ptp1)\ (H_2O)]^{+}$	Cp35	–	SF(7.4) = 6.56 (H)/6.04 (P)	[46]
$[Mn^{II}(Hqp1)\ (H_2O)]^{+}$	Cp36	–	SF(7.4) = 7.99 (H)/6.90 (P)	[46]
$[Mn^{II}(H_2qp2)\ (H_2O)]$	Cp37	–	SF(7.4) = 7.08 (H)/7.00 (P)	[46]
$[Mn^{II}\ (H_3qp2)\ (H_2O)]+$				
Salens				
–	Cp38	+91	MCF_{NBT}(7.8) = 6.19 (P)	[27]
–	Cp39	+159	MCF_{NBT}(7.8) = 6.18 (P)	[27]
–	Cp40	+274	MCF_{NBT}(7.8) = 5.97 (P)	[27]
–	Cp41	+315	MCF_{NBT}(7.8) = 6.00 (P)	[27]
–	Cp42	+454	MCF_{NBT}(7.8) = 5.81 (P)	[27]
–	Cp43	+720	MCF_{NBT}(7.8) = 6.07 (P)	[27]
Bimetallic Cu–Zn and Cu–Cu				
$[Cu^{II}Zn^{II}\ (dien)_2(\mu\text{-Im})](ClO_4)_3$	Cp44	–	MCF_{NBT}(7.8) = 6.81 (P)	[89]
$[Cu^{II}Zn^{II}\ (dien)_2(\mu\text{-Im})](ClO_4)_3$@MCM-41	Cp45	–	MCF_{NBT}(7.8) = 7.79 (P)	[47]
$[Cu^{II}Zn^{II}\ (dien)_2(\mu\text{-Im})](ClO_4)_3$@SBA-15	Cp46	–	MCF_{NBT}(7.8) = 7.40 (P)	[48]
$[Cu^{II}_2(dien)_2(\mu\text{-Im})](ClO_4)_3$	Cp47	–	MCF_{NBT}(7.8) = 6.89 (P)	[89]
$[Cu^{II}_2(dien)_2(\mu\text{-Im})](ClO_4)_3$@MCM-41	Cp48	–	MCF_{NBT}(7.8) = 7.71 (P)	[47]
$[Cu^{II}_2(dien)_2(\mu\text{-Im})](ClO_4)_3$@SBA-15	Cp49	–	MCF_{NBT}(7.8) = 7.37 (P)	[48]
Peptides				

(*continued on next page*)

Table 1 (*continued*)

SOD mimics	Abbreviation	$E_{1/2}$ (mV vs. NHE)	$\log k_{cat}$ ($O_2^{\cdot-}$): $method_{detector}$ (pH) = $\log k_{cat}$(buffer)	References
OCP1- Cu^{II}Ac-PDHKHHKH-NH_2	Pep1	+250	MCF_{XTT}(7.4) = 7.38 (H)	[37]
CATm1-Cu^{II}_2Ac-PHYKHRLH-OH	Pep2	+345	—(no SOD activity, but a catalase activity)	[38]
$Cu^{II}/Cu^{II}_2/Cu^{II}Zn^{II}$ cyclic(HKHGPG)$_2$	Pep3	–	MCF_{NBT}(7.4) = 6.67/6.71/6.92 (T)	[35]
Ac-HAAHVH-NH_2 $[Cu^{II}H_{-1}L5]^+$	Pep4	+202	MCF_{NBT}(7.4) = 7.59 (P)	[31]
Ac-HAAHGH-NH_2 $[Cu^{II}H_{-1}L6]^+$	Pep5	+214	MCF_{NBT}(7.4) = 7.79 (P)	[31]
Ac-HGGHGH-NH_2 $[Cu^{II}H_{-1}L7]^+$	Pep6	+230	–	[31]
Ac-HGGGHGH-NH_2 $[Cu^{II}H_{-1}L8]^+[Cu^{II}H_{-2}L8]$	Pep7	+247	MCF_{NBT}(7.4) = 7.56 (P)	[31]
Ac-HHGH-NH_2 $[Cu^{II}L9]^{2+}[Cu^{II}H_{-1}L9]^+$	Pep8	+313/+264	–	[31]
Ac–S2H3–NH_2 $[Cu^{II}L10]^{2+}[Cu^{II}H_{-1}L10]^+$	Pep9	+293	MCF_{NBT}(7.4) = 7.30 (P)	[31]
Ac–S3H4–NH_2 $[Cu^{II}L11]^{2+}$	Pep10	–	MCF_{NBT}(7.4) = 7.81 (P)	[31]
Cu^{II} Ac-HKHKH-NH_2	Pep11	–	–	[32]
Cu^{II} Ac-HHKHKH-NH_2	Pep12	–	–	[32]
Cu^{II} Ac-KAHEFGHSLGLDHSK-NH_2	Pep13	–	–	[32]
Cu^{II} HADHDHKK-NH_2	Pep14	–	–	[32]
Cu^{II} Ac-RHQAGPPHSHR-NH_2	Pep15	–	–	[32]
Ni^{II} HHDLPCGVY-NH_2	Pep16	–	MCF_{NBT}(7.8) = 4.85 (P)	[33]
Ni^{II} HCDLPHGVY-NH_2	Pep17	–	MCF_{NBT}(7.8) = 3.89 (P)	[33]
$[Ni^{II}L^{3S}(OH_2)]^-$	Pep18	Epa = +724 (100 mV/s)	SF(7.75) = 5.26(H)	[24]
Nanoparticles				
CeO_2 NP	–	–	$MCF_{cyt\ c}$(7.2) = 9.56 (T)[a]	[51]
MnO NP (8 nm size)	–	–	$MCF_{cyt\ c}$(7.4) = 9.38 (P)[a]	[54]
Mn_3O_4 NP	–	–	20 μg/mL eq. 1U/mL SOD[a,b]	[56]
Cu-TBAP nanodots	–	–	12.5% of SOD activity[a,c]	[62]

Half-wave redox potentials ($E_{1/2}$) have been converted and expressed in mV vs. NHE (Normal Hydrogen Electrode) for comparison, with $E_{1/2} = (E_{anodic\ peak} + E_{cathodic\ peak})/2$. The intrinsic activity of the SOD mimics $\log k_{cat}$ ($O_2^{\cdot-}$); hence, the kinetics of reaction with superoxide out of any cellular context [6], is displayed under the form $method_{detector}$(pH) = X (Buffer) indicating method used (MCF, SF, PR, see below), buffer, pH. When several buffers are mentioned: P corresponds to a phosphate buffer whereas H is for HEPES, T is for TRIS buffer, and M for MOPS buffer, concentrations are not shown.

'MCF' refers to the rate of the constant back-calculated from the McCord and Fridovich assay [90]. This assay is a kinetic competitive assay between the SOD mimic studied and a detector. In this assay, superoxide is produced by xanthine oxidase as a slow flow. Several UV–visible detectors have been used in the literature, including nitro blue tetrazolium 'NBT', ferricytochrome *c* 'cyt *c*', 2,3-bis-(2-methoxy-4-nitro-5-sulfophenyl)-2*H*-tetrazolium-5-carboxianilide 'XTT' as a detector. The IC_{50} is the concentration of the SOD mimic that reduces the reaction rate of the detector with superoxide by a factor of 2. Then $k_{cat} = k_{detector}$x[detector]/IC_{50} [6,8,91]. Back-calculating the k_{cat} was only possible when the authors explicitly gave the concentration used for the detector.

'PR' stands for pulsed radiolysis and 'SF' for Stopped-Flow (see Ref. [92] for a comprehensive description of the methodology). Both in PR and SF, a high concentration of superoxide is provided in one go at the beginning of the kinetics measurement.

In these direct methods for the kinetics evaluation (PR or SF), superoxide can be given in excess to the catalyst, ensuring several turnovers are possible. In the MCF assay, which is an indirect assay, the superoxide is provided at a continuous slow rate close to that encountered in biological systems. Indirect and direct methods are thus complementary.

[a] $\log(k_{cat})$ determined per mole NPs.

[b] Method using the production of superoxide with xanthine oxidase and a fluorescent or EPR-based detection, with respectively hydroethidine or 5,5-dimethyl-1-pyridine N-oxide.

[c] MCF-type assay, using superoxide generated upon the UV irradiation of riboflavin and methionine and NBT as a detector.

activity. These two different approaches are described in the sections below.

Loading Cu-M imidazolate-bridged complexes (M = Cu^{II} or Zn^{II}, Cp44 and 47) in silica nanopores of different sizes (MCM-41 [47] or SBA-15 [48], Cp45,46 and 48,49) led to improved catalysis of superoxide dismutation more pronounced in the case of the smallest pores (MCM-41 [47]; see Table 1). The matrix was suggested to maintain Cu and H-Im-Zn(II) in close vicinity in the course of the catalytic cycle [47], during which the imidazolate has been described to decoordinate from Cu(II) upon reduction to Cu(I). Garcia-Espana et al. have grafted hepta-azacyclophane ligands (Cp11,14) in a positively charged boehmite, with a significant enhancement of the antisuperoxide activity [49], as opposed to the negatively charged silica that produced no enhancement (see Table 1). This effect was attributed to the positively charged scaffold, which should help in driving $O_2^{\cdot-}$ to the active site, mimicking the positively charged funnel of native enzymes [23].

Scheme 1

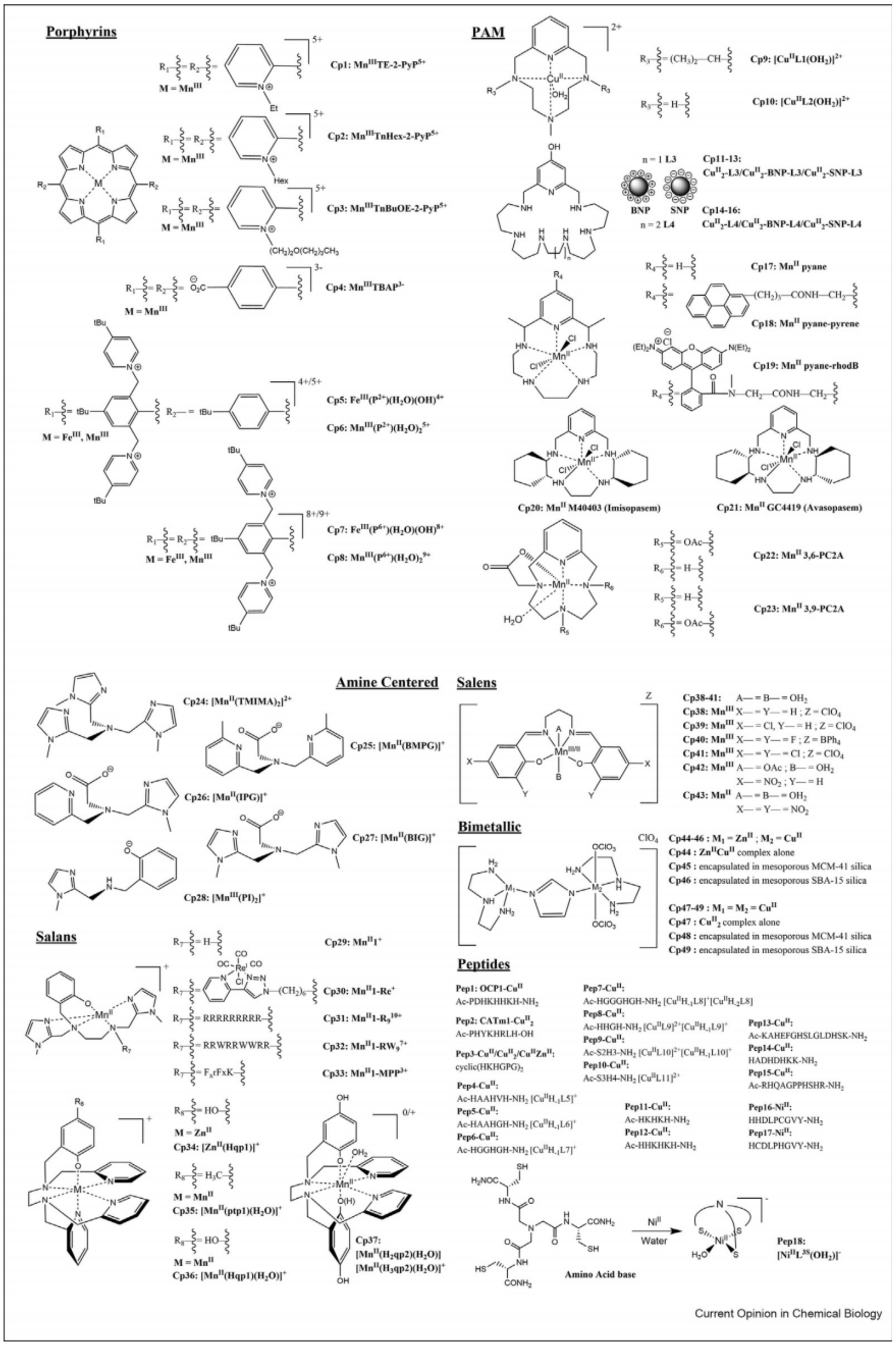

Structures of the SOD mimics mentioned here. Cp stands for compound, Pep for peptides, BNP for boehmite nanoparticles, SNP for silica nanoparticles, S for sarcosyl, MCM-41 for mesoporous MCM-41 silica, SBA-15 for mesoporous SBA-15. Core structures of five SOD mimic families—porphyrins, poly-aza-macrocycles (PAM), ligands amine centered, salan-type ligands, salen-type ligands, bimetallic—are given with variable side chains (R_x). For some of the molecules, the name/code from the original papers is also reminded.

Metal-based nanomaterials display a high density in metal centers that can act as catalytically active redox sites for catalysis [50]. The SOD-like activities of these materials were evaluated qualitatively or reported *per mole of NPs*, as k_{cat} or in the percentage of SOD activity (see Table 1). However, these values are difficult to compare with those determined for molecular catalysts, as there is a high number of accessible catalytic sites per NPs. Nonetheless, these materials display valuable antioxidant activity, approaching those of SOD on a *per mole NPs* basis. After the pioneering work of Self et al. on ceria nanoparticles [51], later encapsulated in various protein scaffolds [52,53], Mn-based nanoparticles (e.g. Mn_3O_4) [54–56] or Fe-based Prussian blue [57–59] were recently characterized for their multiple catalytic activities—SOD, catalase and GSH-peroxidase—possibly retained in cells or *in vivo* [55]. Interestingly, Singh et al. have evidenced that the supernatants of Mn_3O_4 NPs were not active, nicely ruling out the possible involvement of leached ion in the activity [55]. The activities were dependent on the shape and size of the particles [55]. In these condensed systems, the clustering effect of the substrate, proposed in another context [45], could be at stake. Metal–organic frameworks (MOF) have also been used as a scaffold to build metalloenzyme mimics [50], and a few MOF have been designed, either with dispersed copper [61] or using porphyrin (TBAP, see Scheme 1 for the porphyrine acronym) and copper(II) as building blocks [62] with activity reported to 12.5% that of SOD. These MOF are endowed with multiantioxidant activities, but also Fenton pro-oxidant effect [61,62]. Some of these materials have been applied as antioxidants or anti-inflammatory agents [54–57,59,62], others as anticancer agents, their anticancer activity being related to toxicity associated with pro-oxidant effect due to the overproduction of H_2O_2 and/or of HO° [60,61]. Note that similar anticancer activity has also been described for Mn-porphyrins and has already been extensively reviewed [21,63].

Studies in cells: pathways beyond direct antioxidant effects and physicochemical characterization in cells

An indirect mode of action enhancing the antioxidant cellular defenses

Recently, an increasing interest has grown about potential 'side reactions' performed more specifically by Mn-porphyrins (MnPs) with reactive oxygen species (ROS) or cellular compounds ($ONOO^-$, H_2O_2, H_2S, $CO_3^{\bullet-}$, ascorbate, and GSH) [13] and their mechanism of action in cells [7,18,63]. As early as 2004, an increase in extracellular SOD and MnSOD was reported [64] after incubating cells with MnPs, suggesting that these compounds may act not solely as a direct antioxidant by reducing ROS concentration but also indirectly: they may induce antioxidant cell feedback through a pro-oxidant effect, enhancing the protective cell arsenal. Batinic et al. have reported such a pro-oxidant effect of MnPs in 2012 [65,66]. They have extensively shown then that besides their reactions against ROS and reactive nitrogen species (RNS), MnPs display an effect on thiols regulation and cellular sulfur metabolism [7,18,63,67], which activates the Nrf2 [68] pathway. This is interesting as the Keap1-Nrf2 pathway [69,70] constitutes the major defense system against electrophilic and oxidative stress: Keap1 acts as a redox sensor through the oxidation or modification of its cysteine residues upon oxidative/electrophilic stress, which results in the Nrf2-induced up-regulation of several antioxidant enzymes (see Figure 1). It shows that compounds endowed with an overall antioxidant cellular activity may actually be active by the induction of cellular antioxidant feedback via the Keap1-Nrf2 pathway through a pro-oxidant effect. Interestingly, this activation would constitute a late but long-lasting effect, as opposed to an immediate catalytic antioxidant direct effect, but possibly lasting shorter if the antioxidant catalyst is metabolized.

Examples of SOD-mimics inducing this Nrf2 pathway, or not

MnTnBuOE-2-PyP^{5+} (Cp3) is an example of a SOD mimics inducing such an activity. This Mn-porphyrin has been shown to upregulate the expression of enzymes under the control of Nrf2, including NQO1, catalase and MnSOD, through Nrf2 activation in hematopoietic stem cells in transgenic mice [67]. The activation of Nrf2 is suggested to occur via Keap1's S-glutathionylation. Similarly, a polyazamacrocyclic MnSOD mimic, M40403 (Cp20), was shown to increase the expression level of Nrf2 in the skin of diabetic rats [71]. But this scheme is not general. In contrast, the salan-type SOD mimics Cp29-31 reduce the overexpression of mitochondrial MnSOD associated with lipopolysaccharide-induced oxidative stress in intestinal epithelial cells (IECs), indicating that these SOD mimics can complement mitochondrial MnSOD. This result pinpoints a direct antioxidant effect as opposed to an activation of the Nrf2 pathway. No effect on cytosolic CuSOD or catalase was recorded, showing the importance of mitochondria and the specific management of superoxide [41–44].

Detection in cells

The biological efficiency of SOD mimics is linked to their intrinsic SOD activity and also to other parameters such as cellular uptake, subcellular distribution, and speciation in biological environments that are intricate and abound with Lewis bases [6].

Overall cellular uptake of metal complexes can be quantified using techniques such as inductive-coupled plasma mass spectrometry ICP-MS [42,44] whatever the metal ion (Mn, Fe, Cu, Zn, Ni), or specific

Figure 1

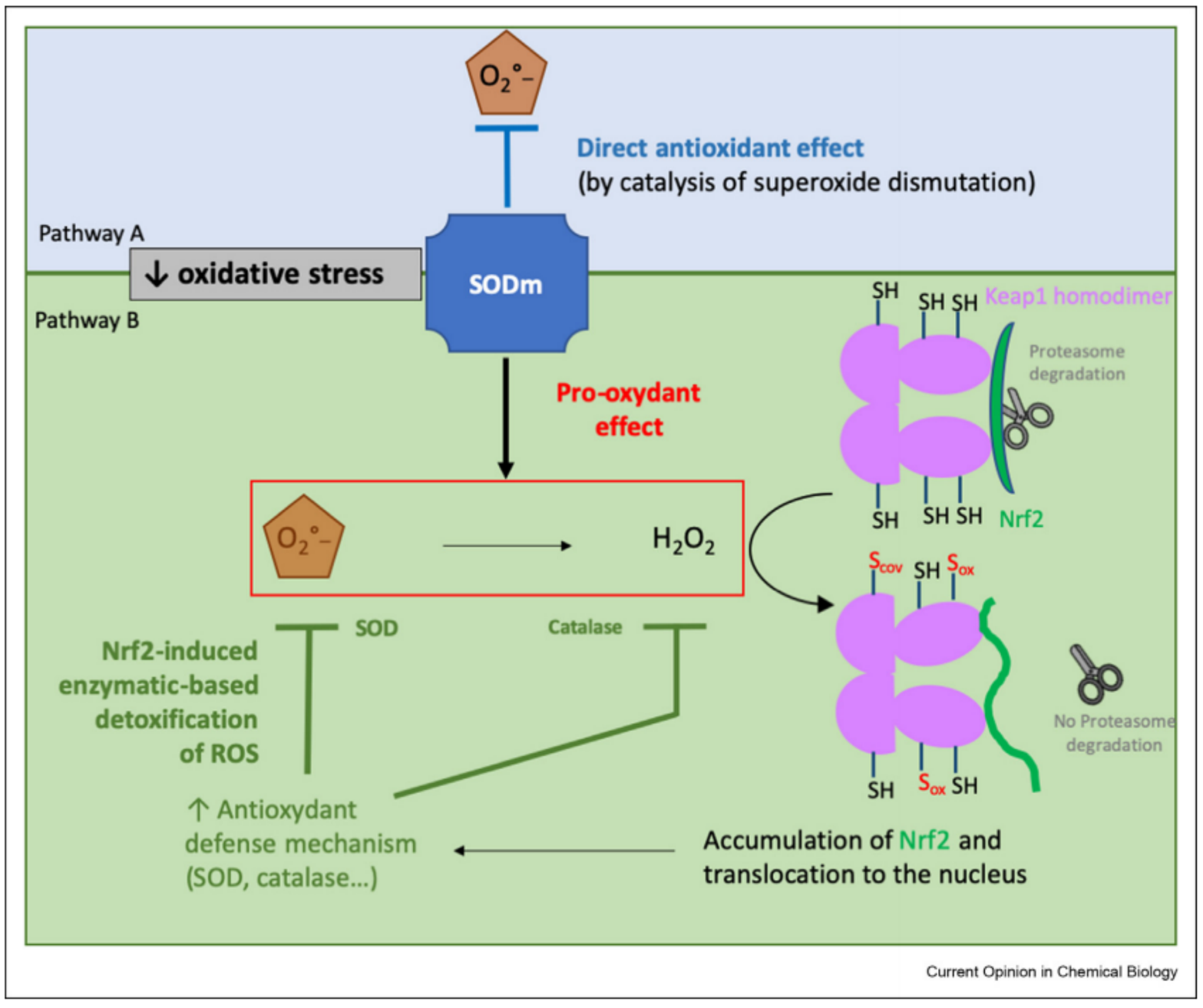

Schematic representation of the two possible pathways from the literature for the SOD mimics cellular activity. Pathway A corresponds to the direct effect of SOD mimics, with their ability to catalytically dismutate superoxide. Pathway B is associated with a pro-oxidant effect of SOD mimics: as they produce H_2O_2, they can activate the Nrf2-signaling pathway. Nrf2 is continuously produced in cells, and Keap1, by binding Nrf2 in a particular conformation, promotes its degradation by the proteasome. Oxidative or chemical stress is sensed by modification of Keap1 cysteines. Their covalent modification/oxidation by electrophiles or oxidants (S_{cov} or S_{ox}) leads to an inhibition of Nrf2 degradation by the proteasome. Nrf2 then accumulates in the cytosol and translocate to the nucleus, where it activates genes of a series of proteins, including antioxidant proteins such as catalase or SODs. The balance between these two pathways depends on the speed of dismutation (k_{cat}) in comparison with the cellular capacity to detoxify H_2O_2 and also on the H_2O_2 content of the cell. Pathway A may occur as soon as the SOD mimics enter the cells or the mitochondria but is also prone to decrease in time due to the SOD mimic degradation. In contrast, Pathway B requires time to activate protein synthesis (from 30 min to several hours), but this has a long-lasting effect as it works by boosting the cellular antioxidant feedback.

techniques such as EPR, available for instance in the case of S = 5/2 Mn^{II} [41–43,72], EPR and ICP-MS estimates being shown to be consistent [42]. In the case of MnPs, UV–vis spectroscopy of cell lysates [44,63,73] also gave estimates similar to ICP-MS [44]. Quantification of MnP in mice tissues, after injection or oral gavage, was performed using LC-MS/MS [74,75], and the trend of their penetration in the brain matched with the lipophilicity, the more lipophilic compounds (MnTnBuOE-2-PyP^{5+} (Cp3), MnTnHex-2-PyP^{5+} (Cp2)) being more concentrated in brain tissues such as cortex and hippocampus, whereas MnTE-2-PyP^{5+} (Cp1) was not detected in the brain. The Mn oxidation state in MnPs was investigated using resonant Raman spectroscopy in the 1250-1550 cm^{-1} range in whole endothelial cells: MnTnBuOE-2-PyP^{5+} (Cp3) and MnTnHex-2-PyP^{5+} (Cp2) were predominantly in their reduced Mn(II) form and present at the mitochondria, as seen by cellular fractionation [76]. The weaker stability of the PMn(II) redox state could make it prone to exchanges with Zn(II) [77,78], which does not seem to occur in cells, probably due to the low bioavailability of Zn(II) being sequestered at the active site of enzymes and mainly in the nucleus. Last but not least, X-ray absorption spectroscopy (XAS) can be used to quantify the relative content of metal complexes directly in cells prepared for X-ray fluorescence microscopy (XFM) (see below) [41,79,80] or in whole-cell pellets (freeze-dried) [79]. Note that applications of XAS and XFM in bioinorganic research have been reviewed recently [81].

Distribution in cells is also a key to the understanding of bioactivity. A first paper showed different cellular distributions for two MnPs. MnTE-2-PyP^{5+} (Cp1) was

Figure 2

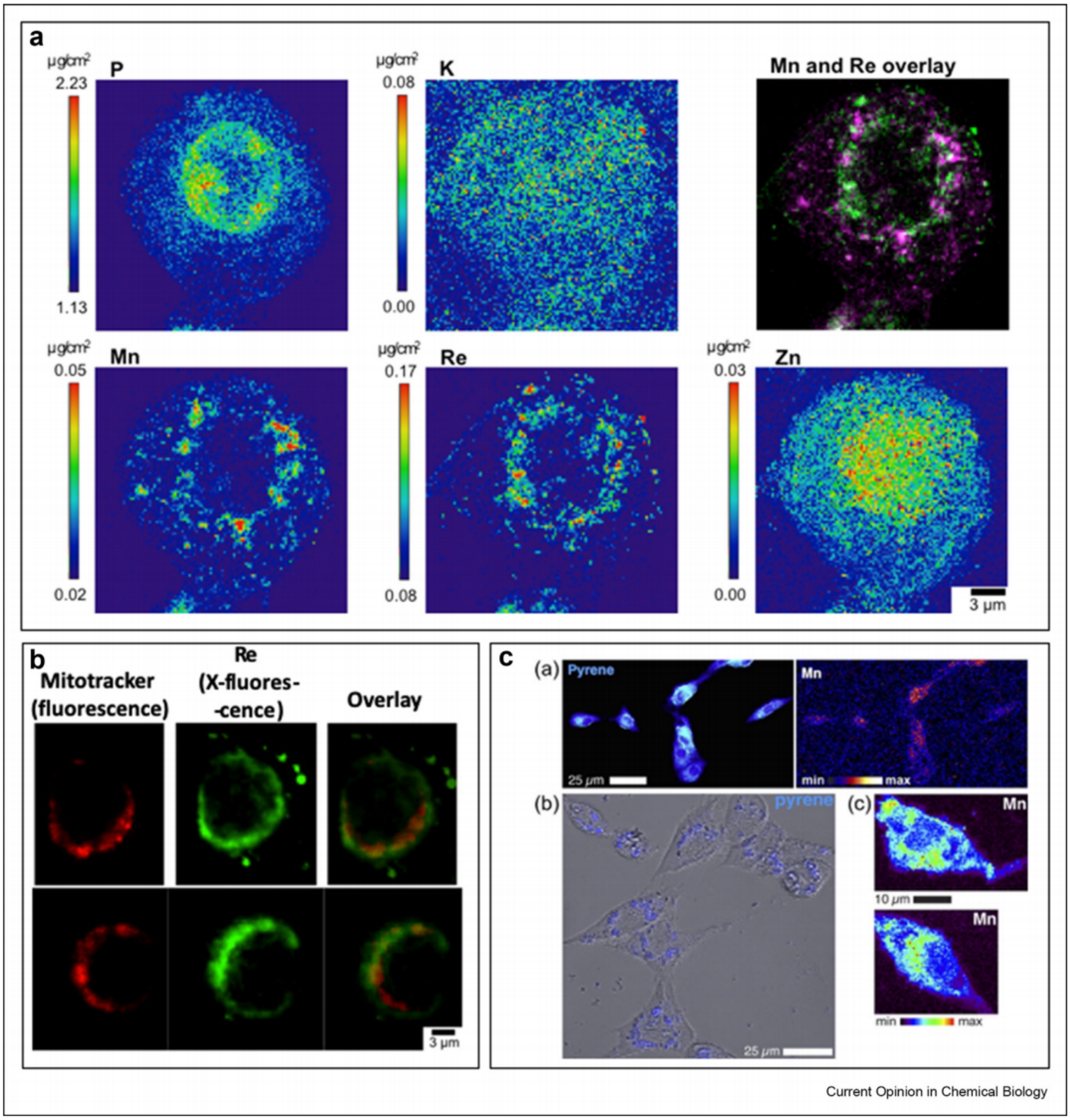

Imaging SOD mimics in cells. **2a.** Elemental distribution of P, K, Mn, Re, and Zn in an HT29-MD2 cell incubated with Cp30. The phosphorus (P) and zinc (Zn, K-lines) maps were used to identify the nucleus area. The overlay (top right) corresponds to the Mn (magenta) and Re (L-lines) (green) maps. The regions corresponding to an overlap of both elements are displayed in white. Intestinal epithelial cells HT29-MD2 were incubated for 2 h with Cp30 (100 µM, 0.02% DMSO) before cryofixation and freeze-drying. Images were recorded on the 2-ID-D beamline of the APS synchrotron (excitation at 12.0 keV chosen to excite both Re and Mn; integration time, 2 s per pixel; pixel size, 200 nm). Scale bar, 3 µm. This figure shows the un-even and punctuated distribution in cells of Cp30. It was colocalized with a Mito Tracker previously mapped in classical fluorescence (not shown). The merging of Re and Mn maps shows areas where Re does not colocalize with Mn, revealing that partial decoordination occurred. **2b.** Confocal fluorescence images of HT29-MD2 cells incubated with a mitochondrial marker (MitotrackerTM, fluorescence) and X-fluorescence maps of Cp30 (Re, X-fluorescence). Intestinal epithelial cells HT29-MD2 were incubated for 1h30 with Cp30 (100 µM, 0.02% DMSO) before the addition of MitotrackerTM deep red (200 nM, 30 min), washing with 50 mM EDTA, cryofixation, and freeze-drying. Confocal fluorescence images of MitotrackerTM deep red (ex 633 nm, em 645–750 nm) were recorded with an open pinhole. X-fluorescence (Re) images were recorded on the Nanoscopium beamline of SOLEIL synchrotron (excitation at 14.1 keV; integration time, 2.4 s/pixel; pixel size, 300 nm). Scale bar, 3 µm. The overlay shows that part of the Re signal overlaps with the MitotrackerTM, suggesting that in these areas, Cp30 is localized in the mitochondria. This correlates with EPR titration that shows an accumulation of Mn in these organelles as compared to control cells, but to a lesser extent than Mn1 (Cp29). **2c.** Distributions of the pyrene tag and manganese, which are similar in SH-SY5Y cells treated with 200 µM Cp18 for 24 h. (a) Fixed cells imaged by both fluorescence microscopy (pyrene tag, left) and low-resolution XFM (manganese, right). (b) Confocal fluorescence microscopy image of the pyrene tag (blue) in living cells (bright field) treated with Cp18. (c) High-resolution elemental maps of manganese in chemically fixed (PFA) cells. Figure 2a and b from Ref. [42] and Figure 2c from Ref. [79].

found evenly distributed, while MnTnHex-2-PyP^{5+} (Cp2), known to be accumulated five times more than MnTE-2-PyP^{5+} in the mitochondria *in vivo* [17,77], displayed a perinuclear distribution within A549 cells [80]. Mathieu et al. have imaged SOD mimics Cp29-33 in freeze-dried HT29-MD2 cells. Whereas Cp29 was homogeneously distributed in cells [41], Cp30 showed a punctuated distribution localized around the nucleus (Figure 2a) [42]. Using quantification (ICP-MS) in a mitochondria-enriched fraction and by colocalization studies with a fluorescent mitochondria-tracker imaged prior to XFM (Figure 2b), Cp30 was found co-localized with this organelle [42]. In a comprehensive paper, Weekley et al. followed a range of Mn-PAMs (Cp17-19), functionalized with a fluorescent probe or not, using XAS of whole cells frozen pellets (see above) and XFM (Figure 2c). Some of the Mn-PAMs were shown to decompose into Mn(II)-phosphate [79]. In both studies [41,79], integration over the cell to determine a range of intracellular concentrations was used, from which a relative scaling for the penetration of various compounds, including $MnCl_2$, was proposed. Mathieu et al. suggested an indirect way to question the speciation of a Mn-complex (Cp30) using XFM imaging, tagging the ligand with heavy metal (by conjugation to a Re-trisCO probe [82]). The Re(ligand) and Mn X-ray fluorescence maps, recorded above the edges of both Re and Mn, were overlapping, but only partly: a few areas showed only Re, revealing some dissociation in cells [42]. In this study, the distribution was also studied both by cell fractionation and XFM, XFM presenting the advantage of fewer steps for sample preparation, which can minimize risks of artefactual contamination or relocalization. Weekley et al. have also studied the distribution of the Mn-PAMs functionalized by a fluorescent probe using both XFM [79] and classical fluorescence (Figure 2c), showing that the fluorescent probes could be cleaved in cells. They conclude with the importance of studying the fate of the complexes in cells.

Conclusion

All these studies highlight the importance of studying SOD mimics in biological environments. Cellular and *in vivo* studies are key to the understanding of their bioactivity, which is a prelude to their therapeutic applications [7,12,14,18,63]. Note that Cp29 was shown to alleviate inflammation in a colitis mice model [41] or reduce the side effects of a treatment by oxaliplatin [83]. Interestingly, Mn-porphyrins (MnTE-2-PyP^{5+} (Cp1) and MnTnBuOE-2-PyP^{5+} (Cp3)) [7] and Mn-PAMs (Cp20-21) [7,84] have advanced to several clinical trials, for anticancer (as sensitizer or radio-protector) or anti-inflammatory applications. Some recent applications of SOD mimics in the context of COVID were investigated to reduce inflammation and cytokine storm [85], undergoing clinical trials (NCT04555096). Overall, the story of SOD mimics and recent developments show that both tool box of the chemists and the knowledge of the cellular and biological pathways are important in the development of compounds mimicking SODs.

Declaration of competing interest

The authors declare that they have no known competing financial interests or personal relationships that could have appeared to influence the work reported in this paper.

Acknowledgments

The authors wish to acknowledge ENS-PSL, PSL, Sorbonne University, CNRS, ANR, and Qlife for financial support. JB thanks the program Interface pour le vivant (IPV-Sorbonne Université) for his PhD fellowship. Fundings for research on the topic of SOD mimics by the research group 'Metals in Biology — Inorganic Biological and Cellular Chemistry' (https://www.chimie.ens.fr/bic/), include the projects MAGIC (ANR-15-CE07-0027), METALLOPEPZYME (ANR-16-CE07-0025-01), CATMAN (ANR 20-CE07-0039-01), MAIN (Qlife initiative, ANR Q-life ANR-17-CONV-0005), DEI20151234413 (Fondation pour la recherche médicale), and BACTMAN and ANACOMDA (Mission pour les initiatives transverses et l'interdisciplinarité-CNRS) and by a research fellowship from the Association François Aupetit (AFA) (associations of French patients suffering from inflammatory bowel diseases).

References

Papers of particular interest, published within the period of review, have been highlighted as:

* of special interest
** of outstanding interest

1. Note that superoxide can also be written $O_2^{\bullet -}$ to stress its radical nature, but this is not mandatory. Similarly, one could write $O_2^{\bullet\bullet}$ to insist on the bi-radical nature of dioxygen, but this is rarely used.

2. Sheng Y, Abreu IA, Cabelli DE, Maroney MJ, Miller A-F, Teixeira M, Valentine JS: **Superoxide dismutases and superoxide reductases**. *Chem Rev* 2014, **114**:3854–3918.

3. Wang Y, Branicky R, Noë A, Hekimi S: **Superoxide dismutases: dual roles in controlling ROS damage and regulating ROS signaling**. *J Cell Biol* 2018, **217**:1915–1928.

4. Gardner PR, Rainer I, Epstein LB, White CW: **Superoxide radical and iron modulate aconitase activity in mammalian cells**. *J Biol Chem* 1995, **270**:13399–13405.

5. Gleason JE, Galaleldeen A, Peterson RL, Taylor AB, Holloway SP, Waninger-Saroni J, Cormack BP, Cabelli DE, Hart PJ, Culotta VC: **Candida albicans SOD5 represents the prototype of an unprecedented class of Cu-only superoxide dismutases required for pathogen defense**. *Proc Natl Acad Sci USA* 2014, **111**:5866–5871.

6. Policar C: **Mimicking SODs, why and how: bio-inspired manganese complexes as SOD mimics**. In *Redox active therapeutics*. Edited by Batinić Haberle I, Rebouças JS, Spasojević I, Springer; 2016:125–164.

7. ** Batinic-Haberle I, Tome ME: **Thiol regulation by Mn porphyrins, commonly known as SOD mimics**. *Redox Biol* 2019, **25**: 101139.
A very comprehensive review on the cellular effects of Mn-porphyrins, covering their diverse non-redox dependent reactivity. In particular, their potential in the modulation of the cellular redox regulatory signaling networks via proteins S-glutathionylation is delineated.

8. Durot S, Policar C, Cisnetti F, Lambert F, Renault J-P, Pelosi G, Blain G, Korri-Youssoufi H, Mahy J-P: **Series of Mn complexes based on N-centered ligands and superoxide – reactivity in**

an anhydrous medium and SOD-like activity in an aqueous medium correlated to MnII/MnIII redox potentials. *Eur J Inorg Chem* 2005, **2005**:3513–3523.

9. Barrette WC, Sawyer DT, Fee JA, Asada K: **Potentiometric titrations and oxidation-reduction potentials of several iron superoxide dismutases**. *Biochemistry* 1983, **22**:624–627.

10. Koppenol WH, Stanbury DM, Bounds PL: **Electrode potentials of partially reduced oxygen species, from dioxygen to water**. *Free Radic Biol Med* 2010, **49**:317–322.

11. Robinett NG, Peterson RL, Culotta VC: **Eukaryotic copper-only superoxide dismutases (SODs): a new class of SOD enzymes and SOD-like protein domains**. *J Biol Chem* 2018, **293**:4636–4643.

12. Batinic-Haberle I, Tovmasyan A, Roberts ERH, Vujaskovic Z, Leong KW, Spasojevic I: **SOD therapeutics: latest insights into their structure-activity relationships and impact on the cellular redox-based signaling pathways**. *Antioxidants Redox Signal* 2014, **20**:2372–2415.

13. Batinic-Haberle I, Tovmasyan A, Spasojevic I: **An educational overview of the chemistry, biochemistry and therapeutic aspects of Mn porphyrins – from superoxide dismutation to H2O2-driven pathways**. *Redox Biol* 2015, **5**:43–65.

14. Bonetta R: **Potential therapeutic applications of MnSODs and SOD-mimetics**. *Chem Eur J* 2018, **24**:5032–5041.

15. Iranzo O: **Manganese complexes displaying superoxide dismutase activity: a balance between different factors**. *Bioorg Chem* 2011, **39**:73–87.

16. Signorella S, Palopoli C, Ledesma G: **Rationally designed mimics of antioxidant manganoenzymes: role of structural features in the quest for catalysts with catalase and superoxide dismutase activity**. *Coord Chem Rev* 2018, **365**:75–102.

17. Miriyala S, Spasojevic I, Tovmasyan A, Salvemini D, Vujaskovic Z, St Clair D, Batinic-Haberle I: **Manganese superoxide dismutase, MnSOD and its mimics**. *Biochim Biophys Acta (BBA) - Mol Basis Dis* 2012, **1822**:794–814.

18. Olson KR, Gao Y, Steiger AK, Pluth MD, Tessier CR, Markel TA, Boone D, Stahelin RV, Batinic-Haberle I, Straubg KD: **Effects of manganese porphyrins on cellular sulfur metabolism**. *Molecules* 2020, **25**:980.

19. Batinić-Haberle I, Tovmasyan A, Spasojević I: **Mn porphyrin-based redox-active therapeutics**. In *Redox-active therapeutics*. Edited by Batinić-Haberle I, Rebouças JS, Spasojević I, Springer International Publishing; 2016:165–212.

20. Batinić-Haberle I, Rebouças JS, Spasojević I: **Superoxide dismutase mimics: chemistry, pharmacology, and therapeutic potential**. *Antioxidants Redox Signal* 2010, **13**:877–918.

21. Batinic-Haberle I, Tovmasyan A, Huang Z, Duan W, Du L, Siamakpour-Reihani S, Cao Z, Sheng H, Spasojevic I, Alvarez Secord A: **H2O2-Driven anticancer activity of Mn porphyrins and the underlying molecular pathways**. *Oxid Med Cell Longev* 2021, **2021**:1–23.

22. Garda Z, Molnár E, Hamon N, Barriada JL, Esteban-Gómez D, Váradi B, Nagy V, Pota K, Kálmán FK, Tóth I, *et al.*: **Complexation of Mn(II) by rigid pyclen diacetates: equilibrium, kinetic, relaxometric, density functional theory, and superoxide dismutase activity studies**. *Inorg Chem* 2021, **60**:1133–1148.

23. ** Martínez-Camarena Á, Llinares JM, Domenech-Carbó A, Alarcón J, García-España E: **A step forward in the development of superoxide dismutase mimetic nanozymes: the effect of the charge of the surface on antioxidant activity**. *RSC Adv* 2019, **9**:41549–41560.
An 8-fold enhancement in SOD activity was demonstrated with several binuclear Cu^{2+} azacyclophanes complexes were grafted onto boehmite nanoparticles. This effect was attributed to their positive ζ-potential since no similar outcome was observed with silica nanoparticles having a negative ζ-potential. The reproduction of the positively charged funnel of native SODs to attract superoxide seems to be a promising strategy to improve the SODm abilities of existing mimics.

24. Domergue J, Pécaut J, Proux O, Lebrun C, Gateau C, Le Goff A, Maldivi P, Duboc C, Delangle P: **Mononuclear Ni(II) complexes with a S3O coordination sphere based on a tripodal cysteine-rich ligand: pH tuning of the superoxide dismutase activity**. *Inorg Chem* 2019, **58**:12775–12785.

25. Kenkel I, Franke A, Dürr M, Zahl A, Dücker-Benfer C, Langer J, Filipović MR, Yu M, Puchta R, Fiedler SR, *et al.*: **Switching between inner- and outer-sphere PCET mechanisms of small-molecule activation: superoxide dismutation and oxygen/superoxide reduction reactivity deriving from the same manganese complex**. *J Am Chem Soc* 2017, **139**:1472–1484.

26. * Franke A, Scheitler A, Kenkel I, Lippert R, Zahl A, Balbinot D, Jux N, Ivanović-Burmazović I: **Positive charge on porphyrin ligand and nature of metal center define basic physicochemical properties of cationic manganese and iron porphyrins in aqueous solution**. *Inorg Chem* 2019, **58**:9618–9630.
The acidity in an aqueous medium of highly charged Mn(P) and Fe(P) (+9 and + 8) with similar redox potentials was found to be different and thought to be important for the protonation of coordinated substrates in the catalytic cycle. In addition to the overall charge to attract negatively charged substrates, the substitutional lability of axial water ligands should play a decisive role in ligand binding for an inner-sphere pathway.

27. Palopoli C, Ferreyra J, Conte-Daban A, Richezzi M, Foi A, Doctorovich F, Anxolabéhère-Mallart E, Hureau C, Signorella SR: **Insights into second-sphere effects on redox potentials, spectroscopic properties, and superoxide dismutase activity of manganese complexes with schiff-base ligands**. *ACS Omega* 2019, **4**:48–57.

28. Martínez-Camarena Á, Sánchez-Murcia PA, Blasco S, González L, García-España E: **Unveiling the reaction mechanism of novel copper *N* -alkylated tetra-azacyclophanes with outstanding superoxide dismutase activity**. *Chem Commun* 2020, **56**:7511–7514.

29. Guijarro L, Inclán M, Pitarch-Jarque J, Doménech-Carbó A, Chicote JU, Trefler S, García-España E, Garcí́a-España A, Verdejo B: **Homo- and heterobinuclear Cu $^{2+}$ and Zn $^{2+}$ complexes of ditopic aza scorpiand ligands as superoxide dismutase mimics**. *Inorg Chem* 2017, **56**:13748–13758.

30. Maroz A, Kelso GF, Smith RAJ, Ware DC, Anderson RF: **Pulse radiolysis investigation on the mechanism of the catalytic action of Mn(II)–Pentaazamacrocycle compounds as superoxide dismutase mimetics**. *J Phys Chem* 2008, **112**:4929–4935.

31. Csire G, Timári S, Asztalos J, Király JM, Kiss M, Várnagy K: **Coordination, redox properties and SOD activity of Cu(II) complexes of multihistidine peptides**. *J Inorg Biochem* 2017, **177**:198–210.

32. Dancs Á, Selmeczi K, Árus D, Szunyogh D, Gajda T: **Catechol oxidase and SOD mimicking by copper(II) complexes of multihistidine peptides**. *Int J Pept Res Therapeut* 2018, **24**:571–575.

33. Lihi N, Kelemen D, May NV, Fábián I: **The role of the cysteine fragments of the nickel binding loop in the activity of the Ni(II)-Containing SOD enzyme**. *Inorg Chem* 2020, **59**:4772–4780.

34. Indeed, coordination reduces the conformational space of flexible ligands by imposing a specific conformation. This orde. [date unknown],

35. Kotynia A, Janek T, Czyżnikowska Ż, Bielińska S, Kamysz W, Brasuń J: **The analysis of Cu(II)/Zn(II) cyclopeptide system as potential Cu,ZnSOD mimic center**. *Int J Pept Res Therapeut* 2017, **23**:431–439.

36. Mathieu E, Tolbert AE, Koebke KJ, Tard C, Iranzo O, Penner-Hahn JE, Policar C, Pecoraro V: **Rational de novo design of a Cu metalloenzyme for superoxide dismutation**. *Chem Eur J* 2020, **26**:249–258.

37. * Vincent A, Rodon-Fores J, Tauziet E, Quévrain E, Dancs Á, Conte-Daban A, Bernard A-S, Pelupessy P, Coulibaly K, Seksik P, *et al.*: **An easy-to-implement combinatorial approach involving an activity-based assay for the discovery of a peptidyl copper complex mimicking superoxide dismutase**. *Chem Commun* 2020, **56**:399–402.
A proof-of-concept paper on a combinatorial design for peptide-based SOD mimics. The methodology uses a one-bead-one-compound method and a screen based on a SOD-activity assay. It led to the

discovery of an efficient peptidyl copper complex Pep1 that exhibited good stability, suitable redox potential, and excellent intrinsic activity. Cell assays showed that Pep1 had beneficial effects against oxidative stress. Interestingly, this complex was found to be inactive as a catalase mimic, while another which was selected with a catalase assay (in another paper [38]) was inactive for SOD activity, validating the specificity of the methodology with regards to activity.

38. Coulibaly K, Thauvin M, Melenbacher A, Testard C, Trigoni E, Vincent A, Stillman MJ, Vriz S, Policar C, Delsuc N: **A di-copper peptidyl complex mimics the activity of catalase, a key antioxidant metalloenzyme**. *Inorg Chem* 2021, **60**:9309–9319.

39. ** Ward MB, Scheitler A, Yu M, Senft L, Zillmann AS, Gorden JD, Schwartz DD, Ivanović-Burmazović I, Goldsmith CR: **Superoxide dismutase activity enabled by a redox-active ligand rather than metal**. *Nat Chem* 2018, **10**:1207–1212.

An unusual Zn(II) SODm complex, with a redox-inactive Zn metal center, was shown to exhibit strong superoxide dismutase activity, which was attributed to the redox-active quinol ligand. The antioxidant activity was characterized using: (a) a McCord and Fridovich derived assay, a competitive assay using xanthine–xanthine oxidase to produce a slow flow of superoxide and lucigenin or cytochrome *c* for detection, (b) a DPPH assay to characterize the radical quenching property, and (c) a stopped-flow full kinetics approach, showing that the catalytic reaction was first order in superoxide. A mechanistic pathway (UV–vis and MS) involving Zn(II)-ligand radical species was proposed.

40. Cabelli DE: **Redox activity goes organic**. *Nat Chem* 2018, **10**:1173–1174.

41. ** Mathieu E, Bernard A-S, Delsuc N, Quévrain E, Gazzah G, Lai B, Chain F, Langella P, Bachelet M, Masliah J, *et al.*: **A cell-penetrant manganese superoxide dismutase (MnSOD) mimic is able to complement MnSOD and exerts an antiinflammatory effect on cellular and animal models of inflammatory bowel diseases**. *Inorg Chem* 2017, **56**:2545–2555.

This study on an SOD mimic (**Mn1**) with intestinal epithelial cells (IEC) included its bioactivity and investigation of the intracellular fate (quantification by EPR in acidified cell lysates, localization by micro-X-fluorescence (XFM) in freeze-dried cells, speciation in cell lysates using MS/MS). In IEC activated by LPS, **Mn1** showed anti-inflammatory activity (as measured by IL8 and COX2 levels). An increase in active MnSOD expression upon LPS was recorded, which was not observed by co-incubation of LPS with **Mn1**, indicating that **Mn1** acted as a direct antioxidant and is able to compensate for MnSOD. **Mn1** was also able to reduce inflammation *in vivo* in chemo-induced acute colitis in mice.

42. Mathieu E, Bernard A-S, Quévrain E, Zoumpoulaki M, Iriart S, Lung-Soong C, Lai B, Medjoubi K, Henry L, Nagarajan S, *et al.*: **Intracellular location matters: rationalization of the anti-inflammatory activity of a manganese(ii) superoxide dismutase mimic complex**. *Chem Commun* 2020, **56**:7885–7888.

43. Mathieu E, Bernard A-S, Ching HYV, Somogyi A, Medjoubi K, Fores JR, Bertrand HC, Vincent A, Trépout S, Guerquin-Kern J-L, *et al.*: **Anti-inflammatory activity of superoxide dismutase mimics functionalized with cell-penetrating peptides**. *Dalton Trans* 2020, **49**:2323–2330.

44. Vincent A, Thauvin M, Quévrain E, Mathieu E, Layani S, Seksik P, Batinic-Haberle I, Vriz S, Policar C, Delsuc N: **Evaluation of the compounds commonly known as superoxide dismutase and catalase mimics in cellular models**. *J Inorg Biochem* 2021, **219**:111431.

45. Wada A, Jitsukawa K, Masuda H: **Superoxide disproportionation driven by zinc complexes with various steric and electrostatic properties**. *Angew Chem Int Ed* 2013, **52**:12293–12297.

46. Senft L, Moore JL, Franke A, Fisher KR, Scheitler A, Zahl A, Puchta R, Fehn D, Ison S, Sader S, *et al.*: **Quinol-containing ligands enable high superoxide dismutase activity by modulating coordination number, charge, oxidation states and stability of manganese complexes throughout redox cycling**. *Chem Sci* 2021, https://doi.org/10.1039/D1SC02465E.

47. * Patriarca M, Daier V, Camí G, Rivière E, Hureau C, Signorella S: **Preparation, characterization and activity of CuZn and Cu2 superoxide dismutase mimics encapsulated in mesoporous silica**. *J Inorg Biochem* 2020, **207**:111050.

Molecular Cu(II)–Zn(II) complexes (Cp44 and Cp47) previously studied as SOD mimics were encapsulated in mesoporous MCM-41 silica. Spectroscopic and magnetic analyses of these materials confirmed the metal centers of the complexes have kept the coordination sphere after insertion into the MCM-41 silica matrix. These complexes@MCM-41 showed a SOD activity increased by one order of magnitude in comparison to the nonencapsulated complexes (see ref. 89). This enhancement SOD was attributed to a matrix effect, the close-fitting of the complexes into the nanochannels of MCM-41 silica favoring the Cu active site and HImZn(or Cu) group to stay in close proximity during catalysis.

48. Patriarca M, Daier V, Camí G, Pellegri N, Rivière E, Hureau C, Signorella S: **Biomimetic Cu, Zn and Cu2 complexes inserted in mesoporous silica as catalysts for superoxide dismutation**. *Microporous Mesoporous Mater* 2019, **279**:133–141.

49. Martínez-Camarena Á, Delgado-Pinar E, Soriano C, Alarcón J, Llinares JM, Tejero R, García-España E: **Enhancement of SOD activity in boehmite supported nanoreceptors**. *Chem Commun* 2018, **54**:3871–3874.

50. Nath I, Chakraborty J, Verpoort F: **Metal organic frameworks mimicking natural enzymes: a structural and functional analogy**. *Chem Soc Rev* 2016, **45**:4127–4170.

51. Korsvik C, Patil S, Seal S, Self WT: **Superoxide dismutase mimetic properties exhibited by vacancy engineered ceria nanoparticles**. *Chem Commun* 2007, https://doi.org/10.1039/B615134E.

52. Liu X, Wei W, Yuan Q, Zhang X, Li N, Du Y, Ma G, Yan C, Ma D: **Apoferritin–CeO_2 nano-truffle that has excellent artificial redox enzyme activity**. *Chem Commun* 2012, **48**:3155–3157.

53. Bhushan B, Gopinath P: **Antioxidant nanozyme: a facile synthesis and evaluation of the reactive oxygen species scavenging potential of nanoceria encapsulated albumin nanoparticles**. *J Mater Chem B* 2015, **3**:4843–4852.

54. Ragg R, Schilmann AM, Korschelt K, Wieseotte C, Kluenker M, Viel M, Völker L, Preiß S, Herzberger J, Frey H, *et al.*: **Intrinsic superoxide dismutase activity of MnO nanoparticles enhances the magnetic resonance imaging contrast**. *J Mater Chem B* 2016, **4**:7423–7428.

55. Singh N, Geethika M, Eswarappa SM, Mugesh G: **Manganese-based nanozymes: multienzyme redox activity and effect on the nitric oxide produced by endothelial nitric oxide synthase**. *Chem Eur J* 2018, **24**:8393–8403.

56. Yao J, Cheng Y, Zhou M, Zhao S, Lin S, Wang X, Wu J, Li S, Wei H: **ROS scavenging Mn_3O_4 nanozymes for *in vivo* anti-inflammation**. *Chem Sci* 2018, **9**:2927–2933.

57. Zhao J, Cai X, Gao W, Zhang L, Zou D, Zheng Y, Li Z, Chen H: **Prussian blue nanozyme with multienzyme activity reduces colitis in mice**. *ACS Appl Mater Interfaces* 2018, **10**:26108–26117.

58. Su L, Xiong Y, Yang H, Zhang P, Ye F: **Prussian blue nanoparticles encapsulated inside a metal–organic framework via in situ growth as promising peroxidase mimetics for enzyme inhibitor screening**. *J Mater Chem B* 2016, **4**:128–134.

59. Zhang W, Hu S, Yin J-J, He W, Lu W, Ma M, Gu N, Zhang Y: **Prussian blue nanoparticles as multienzyme mimetics and reactive oxygen species scavengers**. *J Am Chem Soc* 2016, **138**:5860–5865.

60. Zhu Y, Wang W, Cheng J, Qu Y, Dai Y, Liu M, Yu J, Wang C, Wang H, Wang S, *et al.*: **Stimuli-responsive manganese single-atom nanozyme for tumor therapy via integrated cascade reactions**. *Angew Chem Int Ed* 2021, **60**:9480–9488.

61. Yang P, Tao J, Chen F, Chen Y, He J, Shen K, Zhao P, Li Y: **Multienzyme-mimic ultrafine alloyed nanoparticles in metal organic frameworks for enhanced chemodynamic therapy**. *Small* 2021, **17**:2005865.

62. * Zhang L, Zhang Y, Wang Z, Cao F, Sang Y, Dong K, Pu F, Ren J, Qu X: **Constructing metal–organic framework nanodots as bio-inspired artificial superoxide dismutase for alleviating endotoxemia**. *Mater Horiz* 2019, **6**:1682–1687.

A Cu–Pd@MIL101 MOF pegylated was shown to display a 'multi-enzyme'-like activity, namely, peroxidase from pH 4 to 6, SOD, and capacity to deplete GSH. Its cellular uptake was determined along with the HO° formation under a hypoxic tumor environment. The SOD-like

nanozymes produced a higher flow in H_2O_2. In the tumor environment, where the level of H_2O_2 is close to the toxic threshold, this can lead to toxicity, whereas no toxicity is seen in noncancerous cells, which have a lower level of H_2O_2. The nanozymes showed toxicity for breast cancer cell, with increase in lipid peroxidation, but had no effect on the proliferation of normal cells (HUVEC and LO_2). These nanozymes derived from MOF are thus promising for tumor chemotherapy.

63. Batinic-Haberle I, Tovmasyan A, Spasojevic I: **Mn porphyrin-based redox-active drugs: differential effects as cancer therapeutics and protectors of normal tissue against oxidative injury**. *Antioxidants Redox Signal* 2018, **29**: 1691–1724.

64. Tse HM, Milton MJ, Piganelli JD: **Mechanistic analysis of the immunomodulatory effects of a catalytic antioxidant on antigen-presenting cells: implication for their use in targeting oxidation–reduction reactions in innate immunity**. *Free Radic Biol Med* 2004, **36**:233–247.

65. Jaramillo MC, Briehl MM, Crapo JD, Batinic-Haberle I, Tome ME: **Manganese porphyrin, MnTE-2-PyP5+, acts as a pro-oxidant to potentiate glucocorticoid-induced apoptosis in lymphoma cells**. *Free Radic Biol Med* 2012, **52**:1272–1284.

66. Jaramillo MC, Briehl MM, Batinic-Haberle I, Tome ME: **Manganese (III) meso-tetrakis N-ethylpyridinium-2-yl porphyrin acts as a pro-oxidant to inhibit electron transport chain proteins, modulate bioenergetics, and enhance the response to chemotherapy in lymphoma cells**. *Free Radic Biol Med* 2015, **83**:89–100.

67. ** Zhao Y, Carroll DW, You Y, Chaiswing L, Wen R, Batinic-Haberle I, Bondada S, Liang Y, St Clair DK: **A novel redox regulator, MnTnBuOE-2-PyP5+, enhances normal hematopoietic stem/progenitor cell function**. *Redox Biol* 2017, **12**: 129–138.

Hematopoietic stem/progenitor cells (HSPCs) are known to be sensitive to dioxygen, with a prolonged lifetime under hypoxia. A redox-active SOD-mimic, MnTnBuOE-2-PyP^{5+} (Cp3), which has been shown in an earlier work to accumulate in the mitochondria, was found to increase the number of bone marrow HSPCs in freshly isolated mouse bone marrow cells or mice and to improve the function of long-term engraftment and multilineage differentiation of the HSCs; these can be associated with ROS regulation. MnP also induced a reduction in oxidative phosphorylation. Using an oxidative stress transcription factor activation profiling array and quantification of the protein under Nrf2-control, it was shown that Cp3 (20 μM, 1h, 5% O_2, bone marrow nucleated cell) significantly upregulated the Nrf2/ARE system (ARE = antioxidant response element). These effects suggested that Cp3 acted as a mild pro-oxidant, elevating H_2O_2 in bone marrow cells.

68. Nrf2 stands for nuclear factor erythroid 2-related factor 2. [date unknown],

69. Keap1 stands for Kelch-like ECH-associated protein 1. [date unknown],

70. Yamamoto M, Kensler TW, Motohashi H: **The KEAP1-NRF2 system: a thiol-based sensor-effector apparatus for maintaining redox homeostasis**. *Physiol Rev* 2018, **98**:1169–1203.

71. Jankovic A, Ferreri C, Filipovic M, Ivanovic-Burmazovic I, Stancic A, Otasevic V, Korac A, Buzadzic B, Korac B: **Targeting the superoxide/nitric oxide ratio by L -arginine and SOD mimic in diabetic rat skin**. *Free Radic Res* 2016, **50**:S51–S63.

72. Ash DE, Schramm VL: **Determination of free and bound manganese(I1)in hepatocytes from fed and fasted rats**. *J Biol Chem* 1982, **257**:9261–9264.

73. Spasojevic I, Kos I, Benov LT, Rajic Z, Fels D, Dedeugd C, Ye X, Vujaskovic Z, Reboucas JS, Leong KW, *et al.*: **Bioavailability of metalloporphyrin-based SOD mimics is greatly influenced by a single charge residing on a Mn site**. *Free Radic Res* 2011, **45**: 188–200.

74. Leu D, Spasojevic I, Nguyen H, Deng B, Tovmasyan A, Weitner T, Sampaio RS, Batinic-Haberle I, Huang T-T: **CNS bioavailability and radiation protection of normal hippocampal neurogenesis by a lipophilic Mn porphyrin-based superoxide dismutase mimic, MnTnBuOE-2-PyP5+**. *Redox Biol* 2017, **12**:864–871.

75. Weitner T, Kos I, Sheng H, Tovmasyan A, Reboucas JS, Fan P, Warner DS, Vujaskovic Z, Batinic-Haberle I, Spasojevic I: **Comprehensive pharmacokinetic studies and oral bioavailability of two Mn porphyrin-based SOD mimics, MnTE-2-PyP5+ and MnTnHex-2-PyP5+**. *Free Radic Biol Med* 2013, **58**:73–80.

76. Carballal S, Valez V, Alvarez-Paggi D, Tovmasyan A, Batinic-Haberle I, Ferrer-Sueta G, Murgida DH, Radi R: **Manganese porphyrin redox state in endothelial cells: resonance Raman studies and implications for antioxidant protection towards peroxynitrite**. *Free Radic Biol Med* 2018, **126**:379–392.

77. Spasojević I, Chen Y, Noel TJ, Yu Y, Cole MP, Zhang L, Zhao Y, St Clair DK, Batinić-Haberle I: **Mn porphyrin-based superoxide dismutase (SOD) mimic, MnIIITE-2-PyP5+, targets mouse heart mitochondria**. *Free Radic Biol Med* 2007, **42**:1193–1200.

78. Spasojević I, Chen Y, Noel TJ, Fan P, Zhang L, Rebouças JS, St Clair DK, Batinić-Haberle I: **Pharmacokinetics of the potent redox-modulating manganese porphyrin, MnTE-2-PyP5+, in plasma and major organs of B6C3F1 mice**. *Free Radic Biol Med* 2008, **45**:943–949.

79. ** Weekley CM, Kenkel I, Lippert R, Wei S, Lieb D, Cranwell T, Wedding JL, Zillmann AS, Rohr R, Filipovic MR, *et al.*: **Cellular fates of manganese(II) pentaazamacrocyclic superoxide dismutase (SOD) mimetics: fluorescently labeled MnSOD mimetics, X-ray absorption spectroscopy, and X-ray fluorescence microscopy studies**. *Inorg Chem* 2017, **56**: 6076–6093.

The cellular fate of different MnPAMs, functionalized with fluorescent probes, was studied using XAS (quantification on freeze-dried cells) and XFM (imaging). XAS was used to study speciation in cells. A library of XAS spectra for a range of compounds was collected, and the spectra in cells could be attributed to a combination of Mn^{II}PAMs, $Mn^{III}O$ complexes, and Mn^{II}-phosphate. XFM (Mn maps) was correlated with classical fluorescence (ligands functionalized with a probe), showing that the maps of Mn and ligand could be consistent (Fig1A) or not, pointing to the importance of characterizing the fate of the complexes in cells.

80. Aitken JB, Shearer EL, Giles NM, Lai B, Vogt S, Reboucas JS, Batinic-Haberle I, Lay PA, Giles GI: **Intracellular targeting and pharmacological activity of the superoxide dismutase mimics MnTE-2-PyP^{5+} and MnTnHex-2-PyP^{5+} regulated by their porphyrin ring substituents**. *Inorg Chem* 2013, **52**:4121–4123.

81. Lovett JH, Harris HH: **Application of X-ray absorption and X-ray fluorescence techniques to the study of metallodrug action**. *Curr Opin Chem Biol* 2021, **61**:135–142.

82. Hostachy S, Policar C, Delsuc N: **Re(I) carbonyl complexes: multimodal platforms for inorganic chemical biology**. *Coord Chem Rev* 2017, **351**:172–188.

83. Guillaumot M-A, Cerles O, Bertrand HC, Benoit E, Nicco C, Chouzenoux S, Schmitt A, Batteux F, Policar C, Coriat R: **Oxaliplatin-induced neuropathy: the preventive effect of a new super-oxide dismutase modulator**. *Oncotarget* 2019, **10**: 6418–6431.

84. Anderson CM, Lee CM, Saunders DP, Curtis A, Dunlap N, Nangia C, Lee AS, Gordon SM, Kovoor P, Arevalo-Araujo R, *et al.*: **Phase IIb, randomized, double-blind trial of GC4419 versus placebo to reduce severe oral mucositis due to concurrent radiotherapy and cisplatin for head and neck cancer**. *J Clin Orthod* 2019, **37**:3256–3265.

85. Karlsson JOG, Jynge P, Ignarro LJ: **May mangafodipir or other SOD mimetics contribute to better care in COVID-19 patients?** *Antioxidants* 2020, **9**:971.

86. Batinic-Haberle I, Spasojević I, Hambright P, Benov L, Crumbliss AL, Fridovich I: **Relationship among redox potentials, proton dissociation constants of pyrrolic nitrogens, and in vivo and in vitro superoxide dismutating activities of manganese(III) and iron(III) water-soluble porphyrins**. *Inorg Chem* 1999, **38**:4011–4022.

87. Durot S, Lambert F, Renault J-P, Policar C: **A pulse radiolysis study of catalytic superoxide radical dismutation by a manganese(II) complex with an N-tripodal ligand**. *Eur J Inorg Chem* 2005, **2005**:2789–2793.

88. Ching HYV, Kenkel I, Delsuc N, Mathieu E, Ivanović-Burmazović I, Policar C: **Bioinspired superoxide-dismutase mimics: the effects of functionalization with cationic poly-arginine peptides**. *J Inorg Biochem* 2016, **160**:172–179.

89. Daier VA, Rivière E, Mallet-Ladeira S, Moreno DM, Hureau C, Signorella SR: **Synthesis, characterization and activity of imidazolate-bridged and Schiff-base dinuclear complexes as models of Cu,Zn-SOD. A comparative study**. *J Inorg Biochem* 2016, **163**:162–175.

90. Beauchamp C, Fridovich I: **Superoxide dismutase: improved assays and an assay applicable to acrylamide gels**. *Anal Biochem* 1971, **44**:276–287.

91. Pasternack RF, Halliwell B: **Superoxide dismutase activities of an iron porphyrin and other iron complexes**. *J Am Chem Soc* 1979, **101**:1026–1031.

92. Friedel FC, Lieb D, Ivanović-Burmazović I: **Comparative studies on manganese-based SOD mimetics, including the phosphate effect, by using global spectral analysis**. *J Inorg Biochem* 2012, **109**:26–32.